Characterization of type-2 diacylglycerol acyltransferases in *Haematococcus lacustris* reveals their functions and engineering potential in triacylglycerol biosynthesis and possible roles in astaxanthin esterification

Hongli Cui
Shanxi Agricultural University https://orcid.org/0000-0002-2908-2711
Chunchao Zhao
Shanxi Agricultural University
Wenxin Xu
Shanxi Agricultural University
Hongjiang Zhang
Shanxi Agricultural University
Wei Hang
Shanxi Agricultural University
Xiaoli Zhu
Shanxi Agricultural University
Chunli Ji
Shanxi Agricultural University
Jinai Xue
Shanxi Agricultural University
Chunhui Zhang
Shanxi Agricultural University
Runzhi Li (rli2001@126.com)
https://orcid.org/0000-0002-9933-5024

Research article

Keywords: Haematococcus pluvialis, Diacylglycerol acyltransferase, Function characterization, Triacylglycerol/Astaxanthin, Genetic engineering, Molecular docking

Posted Date: August 19th, 2020

DOI: https://doi.org/10.21203/rs.2.24528/v2

Version of Record: A version of this preprint was published at BMC Plant Biology on January 6th, 2021.
See the published version at https://doi.org/10.1186/s12870-020-02794-6.

Abstract

Background: *Haematococcus lacustris* is an ideal source of astaxanthin (AST) which is stored at oil bodies containing esterified AST (EAST) and triacylglycerol (TAG). Diacylglycerol acyltransferases (DGATs) catalyze the last step of the acyl-CoA-dependent TAG biosynthesis and are also considered as the crucial enzymes involving in EAST biosynthesis in *H. lacustris.* Previous studies have identified four putative DGAT2 encoding genes in *H. lacustris* and only the HpDGAT2D allowed the recovery of TAG biosynthesis, but the engineering potential of HpDGAT2s in TAG biosynthesis, especially possible roles in AST esterification, remains ambiguous.

Results: Five putative DGAT2 genes (HpDGAT2A, 2B, 2C, 2D, and 2E) were identified in *H. lacustris*. Transcription analysis showed that the expression levels of HpDGAT2A, 2B, and 2E genes markedly increased under high light and nitrogen deficient conditions with distinct patterns, which led to significant TAG and EAST accumulation. Functional complementation demonstrated HpDGAT2A, 2B, 2D, and 2E had the capability to restore TAG synthesis in a TAG-deficient yeast strain (H1246) with the large difference in enzymatic activity. Fatty acids (FAs) profiles assays revealed that HpDGAT2A, 2D, and 2E except for 2B preferred monounsaturated fatty acyl-CoA (MUFA) for TAG synthesis in yeast cells, and also showed polyunsaturated fatty acyl-CoA (PUFA) preference by feeding strategy. The over-expression of HpDGAT2D in *Arabidopsis thaliana* and *Chlamydomonas reinhardtii* significantly increased the TAG content and obviously promoted the MUFA and PUFA contents. Interestingly, molecular docking analysis implied that HpDGAT2s structures contained AST binding sites, which provides strong evidence for AST esterification function in *H. lacustris*.

Conclusions: Our study represents a pioneering work on the characterization of HpDGAT2s by systematically integrating expression pattern, AST/TAG accumulation, functional complementation, molecular docking, and over-expression in yeast, plants, and algae. These results (1) update the gene models of HpDGAT2s, (2) prove TAG biosynthesis capacity of HpDGAT2s, (3) show the strong preference for MUFA and PUFA, (4) offer target genes to modulate TAG biosynthesis by genetic engineering method, and (5) provide new evidence for HpDGAT2s roles in AST esterification.

Background

Triacylglycerol (TAG) is the principal storage form of energy in eukaryotic organisms and represents a promising source of biodiesel production [1]. Microalgae can efficiently absorb CO_2 in the atmosphere and turn it into abundant high value products including polysaccharide, lipid, protein, pigment, and biofuel [2-5]. Due to high photosynthetic efficiency, rapid reproduction rate, and short growth cycle, microalgae have been considered as the best candidate to resolve energy crisis and environmental pollution [6]. Further understanding of pathways and regulatory mechanisms involved in TAG accumulation will help benefit the rational genetic manipulation of microalgae [7-9].

Generally, TAG biosynthesis takes place in the endoplasmic reticulum and their assembly can be divided into acyl-CoA-dependent and acyl-CoA independent pathways [10]. Diacylglycerol acyltransferases (DGATs) catalyze the final acylation of sn-1, 2-diacylglycerol (DAG) to form TAG, which is the last and limiting step in the acyl-CoA dependent TAG formation pathway [11]. These enzymes represent a bottleneck in TAG biosynthesis in some oilseed crops and algae, and thus have been regarded as a key target in manipulating TAG production [11]. In higher plants and microalgae, there are four major groups of DGATs: (1) membrane bound form of DGAT1, (2) membrane bound form of DGAT2 sharing low sequence similarity with DGAT1, (3) soluble type of DGAT3 which is localized in the cytosol, and (4) dual functional of WS/DGAT which possess both wax ester and TAG biosynthesis activities [12-18]. DGAT1s are considered to play a critical role in TAGs accumulation in many higher plants and microalgae, whereas DGAT2s appear to have an important role in the formation of TAG containing unusual fatty acids (FAs) [14]. There is strong evidence supporting the involvement of DGAT3 and WS/DGAT in TAG biosynthesis in microalgae [15, 16]. Usually, only one or two copies of DGAT1s are identified in a number of microalgae, whereas multiple copies of DGAT2s are typically present, suggesting that DGAT2s may play an important function in TAG biosynthesis [12-14, 19-27]. Recently, most of the current knowledge about the algal DGATs is derived from the limited algal species including *Chlamydomonas reinhardtii*, *Chlorella ellipsoidea*, *Nannochloropsis oceanica*, *Lobosphaera incise*, *Chlorella/ Chromochloris zofingiensis*, *Myrmecia incise*, and *Phaeodactylum tricornutum*, in which DGATs have been focused on the molecular cloning, biochemical identification, functional characterization, and engineering potential in modulating TAG biosynthesis [19-28]. It is not difficult to find some interesting conclusions that the diversity microalgae are prominent candidates for DGATs and the function of distinct DGATs is unique or species-specific. Therefore, it derived the research interest to other industrially special astaxanthin (AST) producing alga such as *Haematococcus lacustris* [29].

lacustris is a green microalga widely known for its ability to synthesize the highest amount of AST (4% dry weight) under stress conditions [29, 30]. Natural AST is a red-colored carotenoid with strong antioxidant ability and important commercial value [31]. *H. lacustris* is also represented a potential source of TAG, since a considerable increase in TAG content accompanies the accumulation of AST [32-35]. Moreover, the previous studies have indicated that the main form of AST is esterified AST (EAST, 95%) including monoester AST (MAST, 70%) and diester AST (DAST, 25%), which is stored in TAG rich cytosolic oil bodies (OBs) [36-40]. Although the exact mechanisms of stress-induced TAG and AST accumulation in *H. lacustris* are not well understood, several lines of evidence have suggested that the biosynthesis of both compounds appears to be linked through the regulation of oil biosynthetic enzymes at transcription level [40]. Indeed, the accumulation of AST appears to be dependent on the biosynthesis of FAs and accumulation of TAG [34, 41]. In addition, it has been speculated that certain DGATs are the candidate enzymes catalyzing the esterification of AST in *H. pluvialis* [34]. Recently, although four putative type-2 DGATs (HpDGAT2A, B, D and E) were identified from *H. pluvialis* (*lacustris*), and the only HpDGAT2D had the capability of restoring TAG biosynthesis in a TAG-deficient yeast strain [42], but the engineering potential of DGAT2s in TAG biosynthesis, especially roles in AST esterification, remains ambiguous.

By employing the industrially special AST producing alga *H. lacustris*, in the present study, we represented a pioneering work on the characterization of HpDGAT2s by systematically integrating expression pattern, AST/TAG accumulation, functional complementation, molecular docking, and over-expression in yeast, plants, and algae. Five putative HpDGAT2s were identified in *H. lacustris*, of which, the transcription levels of HpDGAT2 genes markedly increased under high light (HL) and nitrogen deficient (ND) conditions with distinct patterns, which led to significant TAG and EAST accumulation. HpDGAT2A, 2D, and 2E rather than 2B had strong TAG biosynthesis activity and preferred monounsaturated fatty acyl-CoA (MUFA) and polyunsaturated fatty acyl-CoA (PUFA). Over-expression experiments indicated the engineering potential of HpDGAT2D in modulating TAG accumulation and FAs composition in algae and plants. We also discussed the roles of HpDGAT2s in AST esterification.

Results

Molecular cloning and bioinformatics analysis of HpDGAT2s genes

Based on the *H. lacustris* transcriptome database [43], five putative DGAT2 genes were predicted by BLAST method using other DGAT2s from different algal species (Additional file 1: Table S1) as query. The full-length mRNA sequences of the five genes were obtained by rapid amplification of cDNA ends (RACEs) method, and the initiation codon, termination codon, 5'-untranslated region (5'-UTR), 3'-untranslated region (3'-UTR), and poly (A) characteristic tail were determined. Five putative DGAT2 genes were designed HpDGAT2A, 2B, 2C, 2D, and 2E by multiple sequence alignment with CrDGAT2s, four of which, HpDGAT2A, 2B, 2D, and 2E contained full-length open reading frame (ORF) while HpDGAT2C was partial sequence (Additional file 2: Table S2 and Additional file 3: Table S3). Then, the full-length ORF were cloned and sequenced by PCR with primers (Additional file 4: Table S4), which was renamed and deposited in NCBI GenBank (HpDGAT2A: MT875161; HpDGAT2B: MT875162; HpDGAT2C: MT875163; HpDGAT2D: MT875164; HpDGAT2E: MT875165). This is so far the highest dose of DGAT2s reported in green alga *H. lacustris*. Comparison with gene models of HpDGAT2s reported by Nguyen et al. [42], our results confirmed that there were five HpDGAT2s members in *H. lacustris*. Generally, only one or two copies of DGAT1s are identified in a number of microalgae, whereas multiple copies of DGAT2s are typically present [14].

To gain insights into the biochemical characteristics of HpDGAT2s, the molecular weight (MW), isoelectric point (pI), sub-cellular location, trans-membrane domain (TM), signal peptide (SP), chloroplast transfer peptide (CTP), and phosphorylation site (Phos) were analyzed. No SP or CTP was present in HpDGAT2s protein sequences except for CTP in HpDGAT2C (Additional file 2: Table S2). There were two TMs in all pDGAT2s protein sequences except for three TMs in HpDGAT2B (Additional file 2: Table S2 and Additional file 5: Figure S1), which is consistent with the membrane bound forms of DGAT1 and DGAT2 [14]. In addition, 14-30 phosphorylation sites were predicted in HpDGAT2s protein sequences (Additional file 2: Table S2 and Additional file 6: Figure S2), indicating phosphorylation plays important roles in DGAT2s enzymes activity due to it has been indicated that the DGAT1 enzyme activity was affected by serine phosphorylation sites in mouse DGAT1 [44], TmDGAT1 [45], and BnDGAT1 [46]. It

remains to be determined whether these phosphorylation sites are important for the functional regulation of HpDGAT2 in *vivo*.

To further analysis the conserved domains (CDs) and evolutionary relationship between HpDGAT2s and other algal DGAT2s, multiple sequence alignment and phylogenetic tree were reconstructed. CDs analysis showed that HaeDGAT2s contained 7 CDs [26, 47, 48, including YF/YFP block (CD1) which is essential for DGAT2 activity, HPHG/EPHS block (CD2) which is proposed to partially consist of the active site, PxxR (x=random amino acid) block (CD3), xGGxAE block (CD4), RxGFx(K/R)xAxxxGxx(L/V)VPxxxFG block (CD5) which is the longest conserved sequence in plants and animal, PxxxVVGxPIxVP block (CD6), and RHK block (CD7) (Additional file 7: Figure S3). As shown in Additional file 7: Figure S3, there were two completely conserved amino acid residues (P and F) among all DGAT2s, which is consistent with previous reports that these two highly conserved residues maybe located at the active sites of the enzymes and make significant contribution to the enzymatic activities [49]. The phylogenetic analysis of the HpDGAT2s and other DGATs orthologs from eukaryotic algae and plants was illustrated in Additional file 8: Figure S4, which is consistent with most of previous results [20-26]. Briefly, all HpDGAT2s clustered with the algal DGAT2s orthologs, which are distinct from other DGAT subfamilies including DGAT1, DGAT3, and DGAT/WSD. Of the five HpDGAT2s, HpDGAT2A formed monophyletic subgroup (BS: 100%) with CrDGAT2A, CzDGAT2A, CzDGAT2B, LiDGAT2A, and LiDGAT2B. HpDGAT2B and HpDGAT2E were highly close (BS: 98%) to CrDGAT2B, CzDGAT2E and CrDGAT2C. HpDGAT2C was evolutionary close (BS: 100%) with CzDGAT2C and LiDGAT2C. HpDGAT2D built monophyletic subgroup (BS: 73%) with CrDGAT2D and CzDGAT2D.

AST/TAG accumulation and HpDGAT2 genes transcription expression upon HL and ND stresses

High light (HL) and nitrogen deficient (ND) stresses can effectively promote the accumulation of AST and TAG in *H. lacustris* [32-34, 50-53]. To understand the relationship between HpDGAT2s expression and TAG/AST biosynthesis, time-course patterns of algal biomass, transcription expression, total AST (T-AST), and total TAG (T-TAG) contents in photoautotrophic cultures of *H. lacustris* under HL, ND, and double HL+ND stresses were studied (Fig. 1).

As shown in Fig. 1a, compare to the control experiment, HL (white and blue), ND (1/4N), and double HL+1/4N stresses intensively inhibited the algal growth and the biomass content maintained constant, which was lower than that of control. The T-AST production and composition were summarized in Fig. 1b-1e. The F-AST contents under HLW-1/4N and HLB-1/4N firstly increased on 1 d and then decreased along with the induction time (2-4 d). While F-AST contents under HLW and HLB firstly increased on 1 d and then maintained constant along with the induction time (Fig. 1b). M-AST was the major form and the content continuously increased along with the induction time (1-4 d). It reached 33.8, 27.6. 22.3, 23.8, and 22.2 mg/g under HLB-1/4N, HLW-1/4N, 1/4N, HLB, and HLW stresses, respectively, on the final day (Fig. 1c). This similar trend was also present in D-AST contents, while D-AST was not detected on initial day 0 and the values were less than 3.0 mg/g on the final day (Fig. 1d). T-AST contents had a similar trend as M-AST (Fig. 1e). From these above results we could draw some conclusions that (1) M-AST is the main

form, (2) compare to ND stress, HL is more effective in inducing AST accumulation especially blue HL condition, (3) coupled HL and ND dual stimulation might be better choices in improving AST accumulation. T-TAG contents slowly increased from day 1 to 4 d and reached its maximum value of 29.5, 28.7, 25.2, 26.8, and 24.8%, which was 159.5, 155.1, 136.2, 144.9, and 134.1% higher than that of control (Fig. 1f). The effect of distinct HL, ND and double HL-1/4N stresses on TAG and AST accumulation was consistent with previous studies that AST and lipid biosynthesis was enhanced and the former was coordinated with the later biosynthesis under HL and ND conditions [34, 41].

Previous studies have indicated that DGATs enzymes are probably responsible for both AST esterification and TAG biosynthesis in *H. lacutris* [33, 34]. Therefore, the time-course pattern of HpDGAT2s transcription expression was determined to reveal whether these genes were involved in the HL, ND, and HL-1/4N induction processes. As revealed by qRT-PCR results (Fig. 2), upon exposure of *H. lacustris* cells to HLB-1/4N, HLW-1/4N, 1/4N, HL-B, and HL-W stress conditions, the HpDGAT2s genes transcription expression levels exhibited distinct patterns. Of the five HpDGAT2s, the HpDGAT2B and HpDGAT2C expression levels were decreased and maintained constant (Fig. 2b and 2c). The HpDGAT2A, HpDGAT2D, and HpDGAT2E transcription expression levels increased and reached its maximum at 4 d exposure with different patterns, e.g., HpDGAT2A and HpDGAT2E were HL and ND stress dependent (Fig. 2a and 2e), respectively, while the HpDGAT2D was both stresses dependent (Fig. 2d). Obviously, the HpDGAT2s genes were differentially regulated by HL, ND, and double HL-ND induction processes, suggesting that these enzymes were together involved in the AST and TAG biosynthesis. Our findings contributed to the understanding of the algae response to HL and ND, but the mechanism of AST and TAG accumulation in *H. lacustris* remains to be elucidated.

Functional complementation of HpDGAT2s in yeast

To verify the function of the putative HpDGAT2s enzymes, the ORF encoding sequences were cloned (Additional file 4: Table S4) into pYES2.0 plasmid and heterologously expressed, respectively, in the quadruple mutant yeast strain *S. cerevisiae* H1246 (*Δdga1Δlro1Δare1Δare2*) that lacks the activity of TAG synthesis. The mutant type (H1246) yeast can form TAG when at least one of these four genes was expressed. Furthermore, Wild type (INVSc1) and H1246-EV (H1246 harboring empty vector pYES2.0) yeast strains were used as positive and negative controls, respectively.

The expression of HpDGAT2A, HpDGAT2B, HpDGAT2D, and HpDGAT2E restored TAG biosynthesis at different levels in H1246 cells as indicated by the prominent TAG spot on a TLC plate (Fig. 3a). By contrast, HpDGAT2B expression in H1246 cells produced un-conspicuous TAG indicating a nonfunctional encoded protein considering the low transcription expression level in H1246 cells (Fig. 3b) and *H. lacustris* cells (Fig. 2b). Nevertheless, the limited FAs composition in *Saccharomyces cerevisiae* might lead to the low TAG content for HpDGAT2B. The ability of HpDGAT2A, 2B, 2D, and 2E to restore TAG biosynthesis in yeast led us to examine their FAs substrate specificity. As indicated in Fig. 3b and 3c, the HpDGAT2A, 2B, 2D, and 2E genes were heterologously expressed in H1246 and INVSc1 cells. The changes of TAG content and FAs composition of TAG extracted from the transformed H1246 and INVSc1

cells were similar (data not shown). As shown in Fig. 3d, the TAG contents of expressed HpDGAT2A (78.3%) and HpDGAT2B (56.5%) in H1246 cells were lower than those of control (INVSc1 and INVSc1+EV), while were higher than control in HpDGAT2D (108.7%) and HpDGAT2E (122.7%) expressed H1246 cells. To further test the FAs substrate specificity, FAs from the transformed H1246 and INVSc1 cells were analyzed by GC. As shown in Fig. 3d, compare to control, the MUFA (C16:1 and C18:1) abundance increased in HpDGAT2A, HpDGAT2D, and HpDGAT2E expressed H1246 cells at the expense of SFA (C16:0 and C18:0). Such tendency, however at different levels, was observed for almost all transformed lines of H1246 for various DGATs enzymes [20, 23-28].

Considering the limited FAs composition in yeast strains (C16:0, C18:0, C16:1, and C18:1), some PUFA, rich in *H. lacustris*, including C18:2n6, C18:3n3, C18:3n6, and C18:4n3 were tested the substrate specificity for HpDGAT2A, 2B, 2D, and 2E genes by feeding strategy. The HpDGAT2A, HpDGAT2D, and HpDGAT2E had similar tendency that these PUFAs were incorporated into TAG on the expense of C16:1 and C18:1 with the following patterns of C18:2n6 > C18:3n3 > C18:3n6 > C18:4n3 (Fig. 3e). Considering that the C18:2n6 and C18:3n3 were rich in *H. lacustris*, it is reasonable to speculate that these HpDGAT2s may have potential in the C18:2n6 and C18:3n3-enriched TAG production. The HpDGAT2A, 2D, and 2E genes showed more strong preference for PUFA than MUFA, alternative due to the high feeding content of PUFA than endogenous MUFA content. This phenomenon was also confirmed by Zienkiewicz et al (2018) that some PUFA was incorporated into TAG on the expense of 16:1 and 18:1 in LiDGAT1, LiDGAT2.1, LiDGAT2.2, and LiDGAT2.3 expressing yeast [23] and in CzDGAT2C expressing yeast mutant H1246 cells [26] by feeding test. However, FAs profiles of the TAG fraction from yeast cells expressing HpDGAT2B showed no obvious changes, implying an un-functional protein (Fig. 3e).

HpDGAT2D overexpression promotes TAG biosynthesis and its relative MUFA/PUFA abundance in *C. reinhardtii*

In order to investigate the possible biological role of HpDGAT2s and engineering potential to modulate TAG biosynthesis in algae, we generated HpDGAT2D overexpression lines in evolutionary close green algal *C. reinhardtii* CC849. The HpDGAT2D was selected in further experiments due to the relative strong TAG biosynthetic activity in yeast cells (Fig. 3) and high transcription expression level in *H. lacustris* under stress condition (Fig. 2d). Through screening over 20 putative transformants (confirmed by genomic PCR) by qRT-PCR, three overexpression lines, HpDGAT2D-4, HpDGAT2D-7, and HpDGAT2D-9, exhibited the maximum increase in transcription levels (by ~ 5.5-fold higher than the control) under ND condition at a 4-d batch culture with no significant difference in cell growth between the transgenic lines and control (Fig. 4a and 4b). The HpDGAT2D overexpression led to considerable increases (by ~ 1.4-fold) in TAGs content under ND condition (Fig. 4c). HpDGAT2D overexpression also affected the FAs profiles in TAG (Fig. 4c). A significant increase was observed in the MUFA (C16:1 and C18:1) and PUFA (C18:2n6 and C18:3n3) relative abundance accompanied by a significant decrease in SFA (C16:0 and C18:0) and some PUFA (C16:2, C16:3, C18:3n6, and C18:4n3). These results indicated that (1) HpDGAT2D showed more strong preference for MUFA and PUFA than SFA, (2) of all PUFA, HpDGAT2D had the first option to C18:2n6 and C18:3n3 rather than C16:2, C16:3, C18:3n6, and C18:4n3, (3) these preferred substrates

happened to be the type that is enriched in *C. reinhardtii*. This trend was consistent with results from yeast cells by feeding test (Figs. 3d and 3e) and previous studies of NoDGAT1A expression in *C. reinhardtii* UVM4 and CzDGAT1A expression in oleaginous alga *N. oceanica* by Wei et al (2017) and Mao et al (2019) respectively [20, 22].

HpDGAT2D overexpression enhances seed oil content and its relative MUFA/PUFA abundance in *A. thaliana*

To explore HpDGAT2s as a tool to manipulate acyl-CoA pools and to engineer TAG biosynthesis in higher plants, HpDGAT2D was over-expressed in *Arabidopsis thaliana*. Three *A. thaliana* independent expression T2 generation lines (At-HpDGAT2D-3, 6, and 8) were selected for further detailed analysis. The transgenic lines did not show any visible morphological difference from untransformed control *A. thaliana* e.g., 1000-seeds weight (Fig. 5a). The qRT-PCR results showed that the HpDGAT2D transcript was expressed in transgenic lines at different tissue organs including roots, tubers, leaves, siliques, and seeds with distinct extent (Fig. 5b). The transformation of wild type *A. thaliana* with HpDGAT2D resulted in higher (120.0-126.4%) seed TAG content than control (Fig. 5c). Again, further GC analysis of FAs profiles form TAG revealed that PUFA and MUFA significantly increased accompanied by a significant decrease in SFA (Fig. 5c). However, the exact process of change was much more complicated than those in yeast and C. *reinhardtii* cells. Specifically, of SFA, C16:0 and C22:0 decreased while C18:0 and C20:0 maintained stable. Of MUFA and PUFA, HpDGAT2D preferred C18:1, C18:2n6, and C18:3n3 rather than C20:1, C20:2 and C22:1 in TAG biosynthesis. These results were largely in agreement with those in yeast cells (Figs. 3d and 3e) and *C. reinhardtii* cells (Fig. 4c). Guo et al (2017) indicated that the CeDGAT1 gene can stimulate FAs biosynthesis and enhance seed weight and oil content when expressed in *A. thaliana* and *B. napus* [21].

Molecular docking reveals the binding sites between HpDGAT2s and AST structure

Although some studies have indicated that DGATs are likely to be the crucial enzymes involving in EAST biosynthesis in *H. lacustris* [34], so far there is no direct biochemical evidence. Homology modeling is a useful tool for predicting the 3D structure of proteins [54] and AutoDock tools is a powerful method for identifying potential binding sites between 3D structures and ligands [55]. In this study, the docking studies were attempted to explore the binding sites between AST structure and 3D models of HpDGAT2s. SWISS-MODEL server was successful in generating 3D structures for HpDGAT2A, 2B, 2D, and 2E. All four HpDGAT2s protein structures contained possible AST binding sites (Additional file 9-11: Figure S5-S7). The results from HpDGAT2D were elaborated in detail (Fig. 6). The symmetrical half of the AST molecule (C20) was selected in docking process due to on one hand the oversized C40 structure (compare to C16-C22 fatty acids), on the other hand, in fact, AST esterification mainly occurred on the hydroxyl group of a six-membered ring at both ends (Fig. 6b). The symmetrical half of the AST molecule (C20) got docked onto the predicted 3D model of HpDGAT2D as shown in Fig. 6c. Further, molecular interaction studies showed that 3D model of HpDGAT2D had some potential AST binding sites (amino acids) by van der waals force, conventional hydrogen bond, alkyl, Pi-alkyl, and Pi-sigma (Additional file 12: Figure S8).

Meanwhile, some binding sites between fatty acids CoA (C16:1 and C18:1) and 3D model of HpDGAT2D were also predicted (Fig. 6d and 6e), which verifies the reliability of the AutoDock analysis due to these DGAT2 enzymes should include their binding sites.

Discussion

Haemaococcus lacustris is not only able to produce a substantial amount of TAG but also the highest content of AST under stress conditions, which represents a leading algal candidate of industrial potential [29-35]. For example, HL and ND stresses can effectively promote the accumulation of AST and TAG in *H. lacustris* [32-34, 50-53]. Our results also revealed that (1) T-AST and T-TAG contents significantly increased under HL-W, HL-B, 1/4N, HL-W+1/4N, and HL-B+1/4N conditions, respectively, which was consistent with previous study [34, 41], (2) M-AST was the main form which is also proven by previous studies [36-39], (3) compared to ND stress, HL was more effective in inducing AST accumulation especially under the blue HL condition, which has been testified in our previous study [50], (4) coupled HL and ND dual stimulation might be better choices in improving AST and TAG accumulation in *H. lacustris* (Fig. 1) [53]. Zhang et al (2018) indicated that HL intensity synergizes with ND can effectively stimulate the biosynthesis of AST [53]. The previous studies have indicated that AST is predominantly esterified with FAs and three forms of AST are present, and the main form of AST is EAST (MAST, 70% and DAST, 25%), which is stored in TAG-rich cytosolic oil bodies (OBs) in *H. lacustris* [36-39]. Although the exact mechanisms of stress-induced TAG and AST accumulation in *H. lacustris* are largely unknown, several lines of evidence have implied that the biosynthesis of TAG and AST appears to be linked by the regulation of oil biosynthetic enzymes at transcription level [40]. Therefore, elucidating the stress induced TAG and EAST biosynthetic pathway is crucial to the improvement in the production in *H. lacustris*. In addition, the AST accumulation is found to be dependent by the FAs biosynthesis and TAG accumulation in *H. lacustris* [34, 41]. Recently, Zhang et al (2019) reported that synthesized AST was esterified mainly with the fatty acid C18:1 and stored in TAG filled lipid droplets in *C. zofingiensis* [40]. Unlike in *H. lacustris*, although AST accumulated in a well-coordinated manner with TAG, which is supported by the coordinated up-regulation of both biosynthetic pathways at the transcriptional level, AST is ketolated from zeaxanthin independent of FAs synthesis in *C. zofingiensis* [40]. This different result possibly dues to the difference in genetic traits of these two organisms. Anyway, the enzymes involving in EAST biosynthesis in both AST producing algae *H. lacustris* and *C. zofingiensis* are unclear.

DGATs catalyze the terminal step in acyl-CoA-dependent TAG production pathway and represent a key target in manipulating TAG production [11]. At present, DGATs from different algal species have been widely studied, which indicates that the diversity microalgae are prominent candidates for DGATs and the function of distinct DGATs is unique or species-specific [19-28]. Obviously, the HpDGAT2s genes were differentially regulated by HL, ND, and double HL-ND stresses conditions with distinct patterns, suggesting that these enzymes are together involved in the AST and TAG biosynthesis (Fig. 2). Mao et al (2019) indicated that CzDGAT1A, CzDGTT1, CzDGTT5 and CzDGTT8 were all considerably up-regulated by ND with distinct expression patterns [20]. Chen et al (2015) indicated that the transcript level of MiDGAT2A was regulated by ND stress, which lead to TAG accumulation [28]. Our findings contributed to

the understanding of the algae response to HL and ND, and suggested that HpDGAT2s genes might play important roles in AST and TAG accumulation in *H. lacustris*. In addition, the previous studies have indicated that DGATs are the possible candidate enzymes involvement in both TAG and EAST accumulation [34], which makes it more interesting to identify DGATs in AST producing industrially alga *H. lacustris* [29]. Recently, although four putative type-2 DGATs (HpDGAT2A, B, D and E) were identified from *H. pluvialis* (*lacustris*), and the only HpDGAT2D had the capability of restoring TAG biosynthesis in a TAG-deficient yeast strain [42], but the engineering potential of DGAT2s in TAGs biosynthesis, especially roles in AST esterification, remains ambiguous.

In this study, we demonstrated that there were five DGAT2s in the alga and renamed as HpDGAT2A, 2B, 2C, 2D and 2E according to sequence alignment and phylogenetic analysis results (Additional file 3: Table S3 and Additional file 8: figure S4), which replenished the previous report of four putative type-2 DGATs in *H. pluvialis* (*lacustris*) transcriptome database and HpDGAT2A is a partial coding sequence [42]. Generally, only one or two copies of DGAT1s are identified in a number of microalgae, whereas multiple copies of DGAT2s are typically present [14]. The numbers of DGAT2s were species-specific in various algal organisms, e.g., *Chlamydomonas reinhardtii* (5), *Nannochloropsis oceanica* (13), *Lobosphaera incise* (3), *Chlorella zofingiensis* (8), *Myrmecia incise* (2), and *Phaeodactylum tricornutum* (4) [20, 23, 24, 26-28]. The subcellular localization prediction revealed the different sub-location of HpDGAT2s (Additional file 2: Table S2), which is in consistence with the subcellular localization prediction of DGATs from the green alga *C. reinhardtii* [24] and *C. zofingiensis* [20]. Two or three TMs were present in all HpDGAT2s (Additional file 2: Table S2 and Additional file 5: Figure S1) implying the members of membrane bound forms of DGAT1 and DGAT2 [14]. Interestingly, abundant phosphorylation sites were predicted in all HpDGAT2s (Additional file 2: Table S2 and Additional file 6: Figure S2), indicating phosphorylation plays important roles in DGAT2s enzymes activity due to it has been proven that the DGAT1 enzyme activity was affected by phosphorylation in mouse DGAT1 [44], BnaDGAT1 [46] and TmaDGAT1 [45]. It remains to be determined whether these phosphorylation sites are important for the functional regulation of HpDGAT2 in vivo. The CDs previously identified in DGAT2 enzymes from higher plants and microalgae [26, 47, 48] were also present in HpDGAT2s but with varying degrees of conservation (Additional file 7: Figure S3) including YF/YFP block (CD1) which is essential for DGAT2 activity, HPHG/EPHS block (CD4) which is proposed to partially consist of the active site, and RxGFx(K/R)xAxxxGxx(L/V)VPxxxFG block (CD5) which is the longest conserved sequence in plant and animal. Some putative lipid binding motifs (FLxLxxx and FVLF blocks) in the mouse DGAT2 were not conserved among HpDGAT2s and algal DGAT2s [47, 48, 56]. Moreover, there were two completely conserved amino acid residues (P and F) among all DGAT2s, which is consistent with previous reports that these two highly conserved residues maybe located at the active sites of the enzymes [49].

To characterize the roles of HpDGAT2s, we cloned and identified the four DGAT2 genes with confirmed full-length coding sequence (Additional file 2: Table S2). Expression in the TAG-deficient yeast strain H1246, a commonly used system for DGAT functional complementation [57], confirmed that all of the HpDGAT2 genes are functional, despite the large difference in enzymatic activity (Fig. 3a). Further functional characterization in yeast showed that HpDGAT2D and HpDGAT2E can increase the TAG

content more than HpDGAT2A and HpDGAT2B, resulting in a significant increase in the TAG content of yeast of 108.7-122.7% (Fig. 3d). Its higher activity provides an alternative candidate of HpDGAT2D and HpDGAT2E to modulating TAG accumulation in algae. However, previous study detected that the only HpDGAT2D had the capability of restoring TAG biosynthesis in a TAG-deficient yeast strain [42]. By contrast, in our study, HpDGAT2B expression in H1246 cells produced un-conspicuous TAG possible due to the limited FAs in *Saccharomyces cerevisiae*. This holds true, at least for CzDGTT1 expressed in yeast, the TAG content increased when feeding of the two free FAs [20]. It is also possible that HpDGAT2B may not a real DGAT but other types of transferase, which cannot be distinguished based only on the sequence data [20]. This phenomenon is usually present in green algae, e.g., CrDGTT1 through CrDGTT3 are functional while CrDGTT4 is not [24], NoDGAT1A rather than NoDGAT1B is functional and CzDGTT1 is functional [20, 22].

DAGs and acyl-CoAs are essential substrates for TAG biosynthesis under the catalysis of DGAT enzymes [20, 22, 24]. The acyl-CoAs substrate specificity was determined by FAs profiles analysis. HpDGAT2s showed their strong preference for MUFA (C16:1 and C18:1) in yeast cells. Such tendency, however at different levels, was observed for almost all transformed lines of H1246 for various DGATs enzymes [20, 23, 24, 26-28]. Considering the limited FAs in yeast cells, some PUFA (e.g., C18:2n6, C18:3n3, C18:3n6, and C18:4n3) that are present in *H. lacustris* but not in yeast cells were selected to test the acyl-CoAs substrate specificity by feeding strategy. Interestingly, all HpDGAT2s except for HpDGAT2B showed their wide range preference for PUFA with distinct patterns in yeast cells, especially for C18:2n6 and C18:3n3 that also rich in *H. lacustris*, indicating that these HpDGAT2s may have potential in the engineering of *H. lacustris* for PUFA-enriched TAG production. This phenomenon was also confirmed by Zienkiewicz et al (2018) that some PUFA was incorporated into TAG on the expense of C16:1 and C18:1 in LiDGAT1, LiDGAT2.1, LiDGAT2.2, and LiDGAT2.3 expressing yeast [23] and CzDGAT2C expressing yeast mutant H1246 cells [26] by feeding test respectively. Consistent with the low transcription expression of HpDGAT2B in algal and yeast cells, feeding test demonstrated the low preference of PUFA, again indicating a nonfunctional encoded protein. Although the acyl-CoAs substrate preference was characterized, the DAGs (prokaryotic and eukaryotic) substrate specificity needed to be elucidated in future.

In order to evaluate the possible biological function and engineering potential to modulate TAG biosynthesis for HpDGAT2s in algae and plants, in the present study, we generated overexpression lines in evolutionary close green algal *C. reinhardtii* CC849 and model plants *A. thaliana*, respectively. It is not surprising that HpDGAT2s overexpression enhanced TAG contents in both *C. reinhardtii* CC849 (by ~ 1.4-fold) and *A. thaliana* (by ~ 1.2-fold). Guo et al (2017) indicated that the CeDGAT1 gene can stimulate FAs biosynthesis and enhance seed weight and oil content when expressed in *A. thaliana* and *B. napus* [21]. Compared to control under ND stress condition, it was also worth noting that the TAG content was significantly increased at a 4 d batch culture for HpDGAT2D overexpression lines under the same stress condition (Fig. 4c), possibly due in part to the high transcription expression level (Fig. 4b). Wei et al (2017) detected that NoDGAT1A expression in *C. reinhardtii* UVM4 had no effect on TAG accumulation under nitrogen-replete condition but TAG enhancement was observed under nitrogen-depleted condition

[22], which possibly due to the difference in genetic traits of distinct organisms. However, Mao et al (2019) declared that CzDGAT1A expression in oleaginous alga *N. oceanica* resulted in a considerable increase (~ 2.8-fold) in TAGs level in the linear growth stage [20]. Consistent with the strong preference for MUFA and PUFA rather than SFA in yeast cells, HpDGAT2D also showed similar trend in *C. reinhardtii*. Specifically, HpDGAT2D had the first option to C16:1, C18:1, C18:2n6 and C18:3n3 rather than C16:2, C16:3, C16:4, C18:3n6, and C18:4n3. Interestingly, these preferred substrates happened to be the type that is enriched in *C. reinhardtii*, indicating the potential in the engineering of *C. reinhardtii* for MUFA/PUFA-enriched TAG production. This trend was also consistent with results from yeast cells by feeding test (Figs. 3d and 3e) and also consistent with previous studies of NoDGAT1A expression in *C. reinhardtii* UVM4 and CzDGAT1A expression in oleaginous alga *N. oceanica* by Wei et al (2017) and Mao et al (2019) respectively [20, 22]. In higher plants, the expression of DGATs generally enhances the oil deposition in developing seeds [58]. For example, a stronger expression of DGAT1 was found in developing seeds than in other tissues in soybeans [59]. However, DGAT1 transcripts were also detected in other plant tissues but most strongly in developing embryos and flower petals [60]. In the current study, HpDGAT2D transcript was expressed in transgenic lines at different tissue organs including roots, tubers, leaves, siliques, and seeds with distinct extent (Fig. 5b). However, the exact process of FAs change was much more complicated than those in yeast and C. *reinhardtii* cells (Fig. 5c). The HpDGAT2D showed strong preference for C18:1, C18:2n6, and C18:3n3 rather than C20:1, C20:2 and C22:1 in TAG biosynthesis, which were largely in agreement with those in yeast cells (Figs. 3d and 3e) and *C. reinhardtii* cells (Fig. 4c). Previous studies have indicated that seed-specific overexpression of EgDGAT2 in *A. thaliana* enhanced the content of PUFA 18:2 and 18:3 in seed TAG, when compared to that from wild-type *Arabidopsis*. In turn, the proportion of 18:0 and 20:0 SFA in seed TAG from EgDGAT2 transgenic lines decreased accordingly [61]. In *Thraustochytrium aureum*, DGAT2 expressing under a strong seed-specific promoter in wild-type *A. thaliana* increased oleic acid content [62]. In addition, transgenic plants showed no other phenotypic differences. Therefore, HpDGAT2D should have great potential for increasing the specific oil production in other oil croups.

Although it has been early suggested that DGATs may be involved in the esterification of AST in *H. lacustris* [34], so far there is no direct biochemical evidence to support this hypothesis. Recently, all ten CzDGATs were expressed in a reconstructed AST-producing yeast strain [63] to examine if these enzymes were responsible for EAST biosynthesis. However, no EAST was detected, indicating the null function of CzDGATs in AST esterification [20]. Considering the difference in genetic traits and AST biosynthetic pathway of both AST-producing algal strains *C. zofingiensis* and *H. lacustris*, it inspires us to study the possible roles of HpDGAT2s in AST esterification. The combination of homology modeling and AutoDock is a powerful tool to identify potential binding sites between HpDGAT2s 3D structures and AST molecular [54, 55]. Some possible binding sites were predicted as shown in Fig. 6 (HpDGAT2D) and Additional file 9-11: Figure S5-S7 (HpDGAT2A, 2B, and 2E), which provides another key clue for functional roles of HpDGAT2s in AST esterification, however, further biological experiments, e.g., the expression of HpDGAT2s in AST-producing yeast, algal, and bacteria strains, are necessary to support this hypothesis in future. Recently, binding sites of potential protease inhibitors of COVID-19 and 3D structure of COVID-19

has been detected using AutoDock [64, 65]. However, compare to the presence of cryo-electron microscopy structure of human DGAT1 in complex with an oleoyl-CoA substrate [66, 67], the absence 3D structures of DGAT2s hampers the accuracy of AudoDock results.

Conclusion

Here, we performed an in-depth characterization of HpDGAT2s by systematically integrating expression pattern, AST/TAG accumulation, functional complementation, molecular docking, and over-expression in yeast, plants, and algae. Five putative DGAT2s genes (HpDGAT2A, 2B, 2C, 2D, and 2E) were identified in *H. lacustris* by BLAST and CD analysis. These DGAT2s genes markedly increased at transcription levels under stress condition, which led to significant TAG and EAST accumulation. Functional complementation demonstrated HpDGAT2A, 2B, 2D, and 2E had the capability to restore TAG synthesis in a TAG-deficient yeast strain (H1246) with the large difference in enzymatic activity. FAs profiles assays revealed that HpDGAT2A, 2D, and 2E except for 2B preferred MUFA for TAG synthesis in yeast cells, and also showed PUFA preference by feeding strategy. The over-expression of HpDGAT2D in wild type *A. thaliana* and *C. reinhardtii* significantly increased the TAG content and also showed strong preference for MUFA and PUFA, indicating the engineering potential for increasing the specific TAG production in plants and algae. Interestingly, molecular docking analysis implied that HpDGAT2s protein structures contained binding sites for symmetrical half of the AST, which provide strong evidence for AST esterification function in *H. lacustris*.

Methods

Algal strain and growth condition

The unicellular algal *Haematococcus lacustris* (FACHB-712) strain was obtained from Freshwater Algae Culture Collection at the Institute of Hydrobiology and maintained at the Institute of Molecular Agriculture and Bioenergy (IMAB), Shanxi Agricultural University. *H. lacustris* was cultivated on 100-mL BBM medium in 250-mL Erlenmeyer flasks. These Erlenmeyer flasks were placed in a plant growth chamber under the culture conditions of 25 μmol/m^2/s light intensity with a diurnal cycle of 12 h light /12 h dark at the temperature 23 ± 1 °C. The culture solution in the flasks was shaken at the fixed time and twice a day. For the HL treatment, after the cultures were dark-adapted for 48 h, the later exponentially growing cultures (biomass content of approximately 200 mg/L) were further transferred into fresh medium under continuous white light (390-770 nm) or blue light (420-500 nm) with a light intensity of 500 μmol/m^2/s without a light/dark cycle, respectively. For the nitrogen deficient (ND, 1/4N) treatment, these pre-cultured and dark induced cells were collected and washed with nitrogen-free BBM medium, and then further transferred into fresh BBM medium with 1/4N under the control culture conditions without a light/dark cycle. For the HL and 1/4N double stresses (HL+1/4N) treatment, these pre-cultured and dark induced cells were transferred into fresh medium with 1/4N under the same continuous white light or blue light, respectively. The cultures under control conditions were used as the control. These pre-cultured and dark induced cells, after centrifugation and washing with sterilized water, were sampled as the starting point

(N-0 day). The cultures were sampled N-1, N-2, N-3, and N-4 day after treatment. The cells were harvested by centrifugation (13,100 g at 4 °C for 5 min) and were washed with PBS prior to storage in liquid nitrogen. For cell dry biomass determination, 20 mL cells culture was collected and washed three times, and then the EP tubes containing cells were dried in a DW3 freeze-drier (Heto Dry Winner, Denmark).

Cloning and bioinformatics analysis of HpDGAT2s

The genes encoding putative HpDGAT2s were predicted and cloned as follow three steps: (1) the local BLAST program was used to predict DGAT2s genes based on the *H. lacustris* transcriptome database by the annotated CzDGAT2s and CrDGAT2s (Additional file 1: Table S1), (2) the rapid amplification of cDNA ends (RACEs) method was used to obtain the full-length mRNA sequences and then determine their transcription start sites, stop sites, and encoding sequences, (3) the open reading frame (ORF) for each HpDGAT2s gene was obtained by PCR method again to construct distinct expression plasmids. All the primers used in this study were listed in Additional file 4: Table S4. The molecular weight (Mw), isoelectronic point (pI), sub-cellular localization, signal peptides (SP), chloroplast transfer peptides (CTP), trans-membrane regions (TM), and phosphorylation site (Phos) of HpDGAT2s were predicted by Compute pI/MW, TargetP, ChloroP, SignalP, TMHMM, and NetPhos tools respectively in ExPASy [68]. HpDGAT2s and other DGATs from plants and algae were aligned using ClustalX [69]. Maximum likelihood trees (Le and Gascuel evolutionary model) of HpDGAT2s and other DGATs proteins were constructed using PhyML [70, 71]. Bootstrap (BS) values were inferred from 400 replicates. Graphical representation and edition of the phylogenetic tree were performed with MEGA5 [72] and TreeDyn (v198.3) [73].

RNA isolation and quantitative real-time PCR

The total RNA was extracted according to the EasySpin RNA Extraction Kit (Aidlab Biotech, Beijing, China). The total RNA concentration was quantified by NanoDrop 2000c (Thermo Scientific, USA). Totally, 2 μg RNA was used to synthesize the first-strand cDNAs by the PrimeScript® RT Enzyme Mix I (TaKaRa DRR047A, China) Kit. It is worth to note that RNA solution should be store at -80 °C if not use immediately. The qRT-PCR was performed as described by our previous study using a 7500 Fast Real-Time PCR System (Applied Biosystems, Waltham, MA, USA) with SYBR Green PCR Master Mix (Invitrogen). The mRNA expression level was normalized using the actin gene as the internal control. All analyses were based on the CT values of the PCR products. The comparative CT method was used to investigate the transcriptional expression levels of HpDGAT2s genes [74].

Functional complementation of HpDGAT2s in the TAG-deficient yeast H1246

The ORFs of HpDGAT2A, 2B, 2D, and 2E were PCR amplified using cDNA as template and cloned into the yeast expression vector pYES2.0 (Invitrogen). After confirmation by restriction enzyme digestion and sequencing, the recombinant pYES2.0-HpDGAT2s plasmids were transformed into the *S. cerevisiae* TAG-producing strain INVSc1 or TAG-deficient quadruple mutant strain H1246 by means of S.c. EasyComp Transformation Kit (Invitrogen). Selection of the transformants was finished by using the synthetic medium without uracil (SC-ura). HpDGAT2s expression induction by galactose was performed as

previously described [20]. The expression of HpDGAT2s genes in yeast strain was verified at the transcript level by qRT-PCR method. For the feeding experiments, yeast cultures were induced as described above but in presence of 1% (w/v) Tergitol NP-40 (Sigma Aldrich, St. Louis, MO, USA) in the medium. At the beginning of induction, the appropriate FAs (C18:2n6, C18:3n3, C18:3n6, and C18:4n3) were added to the culture to a final concentration of 100 μM. Samples at OD600 of 2.5 were harvested for lipid extraction, separation by TLC and analysis by GC.

Over-expression of HpDGAT2D in *C. reinhardtii*

The coding sequence of HpDGAT2D was amplified and cloned into PmlI/BmtI sites of pDB-124 (plasmids were donated by Professor Zhangli Hu from Shenzhen University), followed by sequencing for verification. The resulting plasmid was linearized by XbaI and transformed into the *C. reinhardtii* cc849 strain via the glass beads method [75]. Transformants were selected on Tris-acetate-phosphate (TAP) plates with 10 μg/mL bleomycin (Sigma-Aldrich). The integration of HpDGAT2D into *Chlamydomonas* genome was verified by genomic PCR, and its expression was determined by qRT-PCR. For ND stress, the later exponentially growing *C. reinhardtii* cc849 cells (biomass content of approximately 420 mg/L) were collected and washed with nitrogen-free TAP medium, and then further transferred into fresh TAP medium with 1/4N, and cultured under the conditions of 25 μmol/m^2/s light intensity with a diurnal cycle of 12 h light /12 h dark at the temperature 23 ± 1 °C.

Over-expression of HpDGAT2D in *A. thaliana*

The coding sequence of HpDGAT2D was amplified and cloned into EcoRI/XbaI sites of pCAMBIA1303 to yield pCAMBIA1303-HpDGAT2D. The final binary vector was verified by restriction enzyme digestion and sequencing, and then transferred into *Agrobacterium tumefaciens* strain GV3101 by the freeze-thaw method [76]. *A. thaliana* plants were transformed by vacuum infiltration [77]. T1 generation seeds were selected on hygromycin (50 mg/L), and then the selected transformed plants were transferred to soil. T2 transgenic *A. thaliana* lines were used for seed and oil analyses. The stable integration of the pCAMBIA1301-HpDGAT2D into the genome of transgenic *A. thaliana* was checked by PCR amplification. In the meantime, the expression of HpDGAT2D was determined by qRT-PCR.

Total astaxanthin analysis

For carotenoids analysis, the HPLC method was applied to quantify the contents of all the carotenoids [50, 78]. Briefly, the freeze-dried cells (0.01 g) were ground with liquid nitrogen and extracted with acetone until the cells became colorless. After centrifugation at 13100 × g at 4 °C for 15 min, the supernatant was collected and evaporated under nitrogen gas. Finally, the residue was re-dissolved in 1 mL acetone and filtered through a 0.22-mm Millipore organic membrane (Millipore Co., USA) prior to HPLC analysis. Carotenoids were eluted at a flow rate of 1.2 mL/min with a linear gradient from 100 % solvent A [acetonitrile/methanol/0.1 M Tris-HCl (84:2:14), pH 8.0] to 100 % solvent B [methanol/ethyl acetate (68:32)] for 15 min, followed by 12 min of solvent B. The absorption spectra of the carotenoids ranged from 300 nm to 700 nm (Thermo Scientific UltiMate 3000 HPLC, USA). Peaks were measured at 450 nm.

The contents of F-AST, M-AST, and D-AST were determined using the standard curves of standard carotenoids at known concentrations. The carotenoids standards were purchased from Sigma-Aldrich.

Lipid extraction and fatty acids analysis

The lipid extraction and FAs analysis were all performed according to previously described procedures [21, 79, 80]. Briefly, cellular FAs were extracted by incubating 50 mg of yeast cells or 10 mg freeze-dried algae cells or 10 mg of dried seeds of control and transformed plants in 3 mL of 7.5% (w/v) KOH in methanol for saponification at 70 °C for 4 h. Then the pH was adjusted to 2.0 with HCl. The total lipids were extracted according to a modified version of the Bligh and Dyer method [81], and TAG was separated from the total lipids by thin-layer chromatography (TLC) on Silica Gel 60 plates. The solvents that were used were hexane/diethyl ether/glacial acetic acid (70:30:1, v/v). The lipids were visualized by spraying Primuline (Sigma, 10 mg/100 mL acetone: water (60:40 v/v)) and exposing the plate to UV. Triolein (Sigma) was used as the standard. TAGs were recovered from the TLC plates and then trans-esterified with 5% H_2SO_4 in methanol at 85 °C for 1 h. The fatty acid methyl esters (FAMEs) were extracted with hexane and analyzed by gas chromatography. For quantification of the FAs, an appropriate amount of C17:0 FAME (Sigma) was added as internal standard. FAMEs were analyzed by Agilent GC equipped with a flame ionization detector (FID) and a capillary column (HP-88 100 m × 0.25 mm × 0.2 mm). Nitrogen was used as the carrier gas at a flow rate of 2.64 mL/min. The injection and detector temperatures were both set as 250 °C. The gas chromatograph oven was programmed at an initial temperature of 140 °C for 5 min, and then increased up to 250 °C at a rate of 15°C/min. FA component was estimated according to the retention time of fatty acid standard and data was collected by peak area normalization with C17:0 internal standard.

Molecular docking

Homology modeling is a useful tool for predicting the 3D structure of proteins [54] and AutoDock tools is a powerful method for identifying potential binding sites between 3D structures and ligands [55]. SWISS-MODEL server was used to generate 3D structures for HpDGAT2A, 2B, 2D, and 2E [54]. The output of the predicted model generated as pdb file was downloaded for further analysis and visualized using SPDBV 4.10 [83]. The symmetrical half of the AST molecule (C20) was selected in docking process due to on one hand the oversized C40 structure (compare to C16-C22 fatty acids), on the other hand, in fact, AST esterification mainly occurred on the hydroxyl group of a six-membered ring at both ends. In addition, fatty acids CoA (C16:1 and C18:1) were also used to AutoDock analysis as positive control due to these DGAT2 enzymes should include their binding sites.

Statistical analysis

All experiments were repeated three times to ensure the reproducibility. The data were obtained as the mean value ± SD. Statistical analyses were performed using the SPSS statistical package (SPSS Inc., Chicago, IL, USA). Significant differences between treatments were statistically analyzed by paired-samples t-test .The statistical significances are achieved when $P < 0.01$.

Abbreviations

AST: Astaxanthin; EAST: Esterified astaxanthin; F-AST: Free AST; M-AST: Momoester AST; D-AST: Diester AST; TAG: Triacylglycerol; DGAT: Diacylglycerol acyltransferase; ORF: Open reading frame; RACEs: Rapid amplification of complementary DNA ends; UTR: Untranslated region; HL: High light; ND: Nitrogen deficient; MUFA: Monounsaturated fatty acyl-CoA; PUFA: Polyunsaturated fatty acyl-CoA.

Declarations

Acknowledgements

We acknowledge all the members of the research team for their assistance in the field and laboratory work. We thank Professor Hongyan Zhu from University of Kentucky for helping to polish the language and Professor Zhangli Hu from Shenzhen University for donating pDB124 plasmid.

Authors' contributions

HC and CZ carried out the experiments, analyzed the data and drafted the manuscript. WX and HZ performed the over-expression of HpDGAT2s in yeast, algae and plants. WH and XZ participated in gene cloning and sequence analysis of HpDGAT2s. CJ and JX participated in transcription expression of HpDGAT2s in *H. lacustris* under stress condition. CZ participated in growth and TAG/AST accumulation for *H. lacustris* under stress condition. RL conceived the study, participated in its design and revised the manuscript. All authors read and approved the final manuscript.

Funding

This study was supported by the National Natural Science Foundation of China (31902394), Key Research and Development Planning Project of Shanxi Province (201803D31063), Applying Basic Research Planning Project of Shanxi Province (201801D221250), Key Research and Development Planning Project of Jinzhong City (Y192012), Science and Technology Innovation Planning Project of Shanxi Agricultural University (2018YJ16), Shanxi Province Key Projects of Coal-based Science and Technology (FT-2014-01), Shanxi Scholarship Council of China (2015-064), and the Key Project of the Key Research and Development Program of Shanxi Province, China (201603D312005). The funding bodies were not involved in the design of the study, collection, analysis, and interpretation of data, and in writing the manuscript.

Availability of data and materials

Datasets used in the current study are available from the corresponding author on reasonable request.

Ethics approval and consent to participate

Not applicable.

Consent for publication

Not applicable.

Competing interests

The authors declare that they have no competing interests.

Author details

[1]College of Agriculture, Institute of Molecular Agriculture and Bioenergy, Shanxi Agricultural University, Taigu 030801, Shanxi, China

References

1. Giorno F, Mazzei R, Giorno L. Purification of triacylglycerols for biodiesel production from *Nannochloropsis* microalgae by membrane technology. Bioresource Technol. 2013;140:172-8.
2. Bilal M, Rasheed T, Ahmed I, Iqbal HMN. High-value compounds from microalgae with industrial exploitability - A review. Front Biosci. 2017;9:319-42.
3. Hempel F, Maier UG. Microalgae as solar-powered protein factories. Adv Eep Med Biol. 2016;896:241-62.
4. Ma H, Xiong H, Zhu X, Ji C, Xue J, Li R, et al. Polysaccharide from *Spirulina platensis* ameliorates diphenoxylate-induced constipation symptoms in mice. Int J Biol Macromol. 2019;133:1090-101.
5. Ma H, Chen S, Xiong H, Wang M, Hang W, Zhu X, et al. Astaxanthin from *Haematococcus pluvialis* ameliorates the chemotherapeutic drug (doxorubicin) induced liver injury through the Keap1/Nrf2/HO-1 pathway in mice. Food Funct. 2020;11:4659-71.
6. Chen Y, Xu C, Vaidyanathan S. Microalgae: a robust "green bio-bridge" between energy and environment. Crit Rev Biotechnol. 2018;38:351-68.
7. Lenka SK, Carbonaro N, Park R, Miller SM, Thorpe I, Li Y. Current advances in molecular, biochemical, and computational modeling analysis of microalgal triacylglycerol biosynthesis. Biotechnol Adv. 2016;34:1046-63.
8. Goncalves EC, Wilkie AC, Kirst M, Rathinasabapathi B. Metabolic regulation of triacylglycerol accumulation in the green algae: identification of potential targets for engineering to improve oil yield. Plant Biotechnol J. 2016;14:1649-60.
9. Xue J, Niu YF, Huang T, Yang WD, Liu JS, Li HY. Genetic improvement of the microalga *Phaeodactylum tricornutum* for boosting neutral lipid accumulation. Metab Eng. 2015;27:1-9.
10. Bates PD, Browse J. The significance of different diacylgycerol synthesis pathways on plant oil composition and bioengineering. Front Plant Sci. 2012;3:147.

11. Bhatt-Wessel B, Jordan TW, Miller JH, Peng L. Role of DGAT enzymes in triacylglycerol metabolism. Arch Biochem Biophys. 2018;655:1-11.
12. Chen JE, Smith AG. A look at diacylglycerol acyltransferases (DGATs) in algae. J Biotechnol. 2012;162:28-39.
13. Liu Q, Siloto RM, Lehner R, Stone SJ, Weselake RJ. Acyl-CoA:diacylglycerol acyltransferase: molecular biology, biochemistry and biotechnology. Prog Lipid Res. 2012;51:350-77.
14. Xu Y, Caldo KMP, Pal-Nath D, Ozga J, Lemieux MJ, Weselake RJ, et al. Properties and biotechnological applications of acyl-CoA:diacylglycerol acyltransferase and phospholipid:diacylglycerol acyltransferase from terrestrial plants and microalgae. Lipids. 2018;53:663-88.
15. Bagnato C, Prados MB, Franchini GR, Scaglia N, Miranda SE, Beligni MV. Analysis of triglyceride synthesis unveils a green algal soluble diacylglycerol acyltransferase and provides clues to potential enzymatic components of the chloroplast pathway. BMC Genomics. 2017;18:223.
16. Cui Y, Zhao J, Wang Y, Qin S, Lu Y. Characterization and engineering of a dual-function diacylglycerol acyltransferase in the oleaginous marine diatom *Phaeodactylum tricornutum*. Biotechnol Biofuels. 2018;11:32.
17. Li F, Wu X, Lam P, Bird D, Zheng H, Samuels L, et al. Identification of the wax ester synthase/acyl-coenzyme A: diacylglycerol acyltransferase WSD1 required for stem wax ester biosynthesis in *Arabidopsis*. Plant Physiol. 2008;148:97-107.
18. Hernández ML, Whitehead L, He Z, Gazda V, Gilday A, Kozhevnikova E, et al. A cytosolic acyltransferase contributes to triacylglycerol synthesis in sucrose-rescued *Arabidopsis* seed oil catabolism mutants. Plant Physiol. 2012;160:215-25.
19. La Russa M, Bogen C, Uhmeyer A, Doebbe A, Filippone E, Kruse O, et al. Functional analysis of three type-2 DGAT homologue genes for triacylglycerol production in the green microalga *Chlamydomonas reinhardtii*. J Biotechnol. 2012;162:13-20.
20. Mao X, Wu T, Kou Y, Shi Y, Zhang Y, Liu J. Characterization of type I and type II diacylglycerol acyltransferases from the emerging model alga *Chlorella zofingiensis* reveals their functional complementarity and engineering potential. Biotechnol Biofuels. 2019;12:28.
21. Guo X, Fan C, Chen Y, Wang J, Yin W, Wang RR, et al. Identification and characterization of an efficient acyl-CoA:diacylglycerol acyltransferase 1 (DGAT1) gene from the microalga *Chlorella ellipsoidea*. BMC Plant Biol. 2017;17:48.
22. Wei H, Shi Y, Ma X, Pan Y, Hu H, Li Y, et al. A type-I diacylglycerol acyltransferase modulates triacylglycerol biosynthesis and fatty acid composition in the oleaginous microalga, *Nannochloropsis oceanica*. Biotechnol Biofuels. 2017;10:174.
23. Zienkiewicz K, Benning U, Siegler H, Feussner I. The type 2 acyl-CoA:diacylglycerol acyltransferase family of the oleaginous microalga *Lobosphaera incisa*. BMC Plant Biol. 2018;18:298.
24. Liu J, Han D, Yoon K, Hu Q, Li Y. Characterization of type 2 diacylglycerol acyltransferases in *Chlamydomonas reinhardtii* reveals their distinct substrate specificities and functions in

triacylglycerol biosynthesis. Plant J. 2016;86:3-19.

25. Guihéneuf F, Leu S, Zarka A, Khozin-Goldberg I, Khalilov I, Boussiba S. Cloning and molecular characterization of a novel acyl-CoA:diacylglycerol acyltransferase 1-like gene (PtDGAT1) from the diatom *Phaeodactylum tricornutum*. FEBS J. 2011;278:3651-66.
26. Xu Y, Falarz L, Chen G. Characterization of type-2 diacylglycerol acyltransferases in the green microalga *Chromochloris zofingiensis*. J Agr Food Chem. 2019;67:291-8.
27. Gong Y, Zhang J, Guo X, Wan X, Liang Z, Hu CJ, et al. Identification and characterization of PtDGAT2B, an acyltransferase of the DGAT2 acyl-coenzyme A:diacylglycerol acyltransferase family in the diatom *Phaeodactylum tricornutum*. FEBS Lett. 2013;587:481-7.
28. Chen CX, Sun Z, Cao HS, Fang FL, Ouyang LL, Zhou ZG. Identification and characterization of three genes encoding acyl-CoA:diacylglycerol acyltransferase (DGAT) from the microalga *Myrmecia incisa Reisigl*. Algal Res. 2015;12:280-8.
29. Khoo KS, Lee SY, Ooi CW, Fu X, Miao X, Ling TC, et al. Recent advances in biorefinery of astaxanthin from *Haematococcus pluvialis*. Bioresource Technol. 2019;288:121606.
30. Solovchenko AE. Recent breakthroughs in the biology of astaxanthin accumulation by microalgal cell. Photosynth Res. 2015;125:437-49.
31. Shah MM, Liang Y, Cheng JJ, Daroch M. Astaxanthin-producing green microalga *Haematococcus pluvialis*: from single cell to high value commercial products. Front Plant Sci. 2016;7:531.
32. Lei A, Chen H, Shen G, Hu Z, Chen L, Wang J. Expression of fatty acid synthesis genes and fatty acid accumulation in *Haematococcus pluvialis* under different stressors. Biotechnol Biofuels. 2012;5:18.
33. Ma R, Thomas-Hall SR, Chua ET, Alsenani F, Eltanahy E, Netzel ME, et al. Gene expression profiling of astaxanthin and fatty acid pathways in *Haematococcus pluvialis* in response to different LED lighting conditions. Bioresource Technol. 2018;250:591-602.
34. Chen G, Wang B, Han D, Sommerfeld M, Lu Y, Chen F, et al. Molecular mechanisms of the coordination between astaxanthin and fatty acid biosynthesis in *Haematococcus pluvialis* (Chlorophyceae). Plant J. 2015;81:95-107.
35. Kwan TA, Kwan SE, Peccia J, Zimmerman JB. Selectively biorefining astaxanthin and triacylglycerol co-products from microalgae with supercritical carbon dioxide extraction. Bioresource Technol. 2018;269:81-8.
36. Miao F, Lu D, Li Y, Zeng M. Characterization of astaxanthin esters in *Haematococcus pluvialis* by liquid chromatography-atmospheric pressure chemical ionization mass spectrometry. Anal Biochem. 2006;352:176-81.
37. Holtin K, Kuehnle M, Rehbein J, Schuler P, Nicholson G, Albert K. Determination of astaxanthin and astaxanthin esters in the microalgae *Haematococcus pluvialis* by LC-(APCI)MS and characterization of predominant carotenoid isomers by NMR spectroscopy. Anal Bioanal Chem. 2009;395:1613-22.
38. Fábryová T, Tůmová L, Silva DCd, Pereira DM, Andrade PB, Valentão P, et al. Isolation of astaxanthin monoesters from the microalgae *Haematococcus pluvialis* by high performance countercurrent

chromatography (HPCCC) combined with high performance liquid chromatography (HPLC). Algal Res. 2020;49:1247.

39. Pick U, Zarka A, Boussiba S, Davidi L. A hypothesis about the origin of carotenoid lipid droplets in the green algae *Dunaliella* and *Haematococcus*. Planta. 2019;249:31-47.
40. Zhang Y, Ye Y, Ding W, Mao X, Li Y. Astaxanthin is ketolated from zeaxanthin independent of fatty acid synthesis in *Chromochloris zofingiensis*. Plant Physiol. 2020;183:883-97.
41. Zhekisheva M, Zarka A, Khozin-Goldberg I, Cohen Z, Boussiba S. Inhibition of astaxanthin synthesis under high irradiance does not abolish triacylglycerol accumulation in the green alga *Haematococcus pluvialis* (Chlorophyceae). J Phycol. 2005;41:819-26.
42. Nguyen T, Xu Y, Abdel-Hameed M, Sorensen JL, Singer SD, Chen G. Characterization of a type-2 diacylglycerol acyltransferase from *Haematococcus pluvialis* reveals possible allostery of the recombinant enzyme. Lipids. 2019; doi:10.1002/lipd.12210.
43. Gao Z, Li Y, Wu G, Li G, Sun H, Deng S, et al. Transcriptome analysis in *Haematococcus pluvialis*: astaxanthin induction by salicylic acid (SA) and jasmonic acid (JA). Plos One. 2015;10:e0140609.
44. Yu J, Li Y, Zou F, Xu S, Liu P. Phosphorylation and function of DGAT1 in skeletal muscle cells. Biophys Rep. 2015;1:41-50.
45. Xu J, Francis T, Mietkiewska E, Giblin EM, Barton DL, Zhang Y, et al. Cloning and characterization of an acyl-CoA-dependent diacylglycerol acyltransferase 1 (DGAT1) gene from *Tropaeolum majus*, and a study of the functional motifs of the DGAT protein using site-directed mutagenesis to modify enzyme activity and oil content. Plant Biotechnol J. 2008;6:799-818.
46. Caldo KMP, Shen W, Xu Y, Hanley-Bowdoin L, Chen G, Weselake RJ, et al. Diacylglycerol acyltransferase 1 is activated by phosphatidate and inhibited by SnRK1-catalyzed phosphorylation. Plant J. 2018;96:287-99.
47. Liu Q, Siloto RM, Snyder CL, Weselake RJ. Functional and topological analysis of yeast acyl-CoA:diacylglycerol acyltransferase 2, an endoplasmic reticulum enzyme essential for triacylglycerol biosynthesis. J Biol Chem. 2011;286:13115-26.
48. Stone SJ, Levin MC, Farese RV, Jr. Membrane topology and identification of key functional amino acid residues of murine acyl-CoA:diacylglycerol acyltransferase-2. J Biol Chem. 2006;281:40273-82.
49. Cao H. Structure-function analysis of diacylglycerol acyltransferase sequences from 70 organisms. BMC Research Notes. 2011;4:249.
50. Cui H, Yu X, Wang Y, Cui Y, Li X, Liu Z, et al. Evolutionary origins, molecular cloning and expression of carotenoid hydroxylases in eukaryotic photosynthetic algae. BMC Genomics. 2013;14:457.
51. Ding W, Zhao Y, Xu JW. Melatonin: a multifunctional molecule that triggers defense responses against high light and nitrogen starvation stress in *Haematococcus pluvialis*. J Agr Food Chem. 2018;66:7701-11.
52. Recht L, Töpfer N, Batushansky A, Sikron N, Gibon Y, Fait A, et al. Metabolite profiling and integrative modeling reveal metabolic constraints for carbon partitioning under nitrogen starvation in the green algae *Haematococcus pluvialis*. J Biol Chem. 2014;289:30387-403.

53. Zhang WW, Zhou XF, Zhang YL, Cheng PF, Ma R, Cheng WL, et al. Enhancing astaxanthin accumulation in *Haematococcus pluvialis* by coupled light intensity and nitrogen starvation in column photobioreactors. J Microbiol Biotechn. 2018;28:2019-28.
54. Waterhouse A, Bertoni M, Bienert S, Studer G, Tauriello G, Gumienny R, et al. SWISS-MODEL: homology modelling of protein structures and complexes. Nucleic Acids Res. 2018;46:W296-W303.
55. Forli S, Huey R, Pique ME, Sanner MF, Goodsell DS, Olson AJ. Computational protein-ligand docking and virtual drug screening with the AutoDock suite. Nat Protoc. 2016;11:905-19.
56. Zheng L, Shockey J, Bian F, Chen G, Shan L, Li X, et al. Variant amino acid residues alter the enzyme activity of peanut type 2 diacylglycerol acyltransferases. Front Plant Sci. 2017;8:1751.
57. Sandager L, Gustavsson MH, Ståhl U, Dahlqvist A, Wiberg E, Banas A, et al. Storage lipid synthesis is non-essential in yeast. J Biol Chem. 2002;277:6478-82.
58. He X, Turner C, Chen GQ, Lin JT, McKeon TA. Cloning and characterization of a cDNA encoding diacylglycerol acyltransferase from castor bean. Lipids. 2004;39:311-8.
59. Li R, Yu K, Hatanaka T, Hildebrand DF. Vernonia DGATs increase accumulation of epoxy fatty acids in oil. Plant Biotechnol J. 2010;8:184-95.
60. Hobbs DH, Lu C, Hills MJ. Cloning of a cDNA encoding diacylglycerol acyltransferase from *Arabidopsis thaliana* and its functional expression. FEBS Lett. 1999;452:145-9.
61. Jin Y, Yuan Y, Gao L, Sun R, Chen L, Li D, et al. Characterization and functional analysis of a type 2 diacylglycerol acyltransferase (DGAT2) gene from Oil palm (*Elaeis guineensis* Jacq.) mesocarp in *Saccharomyces cerevisiae* and transgenic *Arabidopsis thaliana*. Front Plant Sci. 2017;8:1791.
62. Zhang C, Iskandarov U, Klotz ET, Stevens RL, Cahoon RE, Nazarenus TJ, et al. A thraustochytrid diacylglycerol acyltransferase 2 with broad substrate specificity strongly increases oleic acid content in engineered *Arabidopsis thaliana* seeds. J Exp Bot. 2013;64:3189-200.
63. Zhou P, Ye L, Xie W, Lv X, Yu H. Highly efficient biosynthesis of astaxanthin in *Saccharomyces cerevisiae* by integration and tuning of algal crtZ and bkt. Appl Microbiol Biot. 2015;99:8419-28.
64. Mothay D, Ramesh KV. Binding site analysis of potential protease inhibitors of COVID-19 using AutoDock. VirusDis. 2020;31:1-6.
65. Zhang XY, Huang HJ, Zhuang DL, Nasser MI, Yang MH, Zhu P, et al. Biological, clinical and epidemiological features of COVID-19, SARS and MERS and AutoDock simulation of ACE2. Infect Dis Poverty. 2020;9:99.
66. Wang L, Qian H. Structure and mechanism of human diacylglycerol O-acyltransferase 1. Nature. 2020;581:329-32.
67. Sui X, Wang K, Gluchowski NL, Elliott SD, Liao M. Structure and catalytic mechanism of a human triacylglycerol-synthesis enzyme. Nature. 2020;581:323-8.
68. Gasteiger E, Gattiker A, Hoogland C, Ivanyi I, Appel RD, Bairoch A. ExPASy: the proteomics server for in-depth protein knowledge and analysis. Nucleic Acids Res. 2003;31:3784-8.

69. Thompson JD, Gibson TJ, Higgins DG. Multiple sequence alignment using ClustalW and ClustalX. Curr Protoc Bioinformatics. 2002;Chapter 2:Unit 2.3.
70. Le SQ, Lartillot N, Gascuel O. Phylogenetic mixture models for proteins. Philos Trans R Soc B Sci. 2008;363:3965-76.
71. Guindon S, Dufayard JF, Lefort V, Anisimova M, Hordijk W, Gascuel O. New algorithms and methods to estimate maximum-likelihood phylogenies: assessing the performance of PhyML 3.0. Syst Biol. 2010;59:307-21.
72. Tamura K, Peterson D, Peterson N, Stecher G, Nei M, Kumar S. MEGA5: molecular evolutionary genetics analysis using maximum likelihood, evolutionary distance, and maximum parsimony methods. Mol Biol Evol. 2011;28:2731-9.
73. Chevenet F, Brun C, Bañuls AL, Jacq B, Christen R. TreeDyn: towards dynamic graphics and annotations for analyses of trees. BMC Bioinform. 2006;7:439.
74. Livak KJ, Schmittgen TD. Analysis of relative gene expression data using real-time quantitative PCR and the 2($^{-Delta\ Delta\ C(T)}$) Method. Methods (San Diego, Calif). 2001;25:402-8.
75. Kindle KL. High-frequency nuclear transformation of Chlamydomonas reinhardtii. P Natl Acad Sci USA. 1990;87:1228-32.
76. Holsters M, de Waele D, Depicker A, Messens E, van Montagu M, Schell J. Transfection and transformation of *Agrobacterium tumefaciens*. Mol Gen Genet. 1978;163:181-7.
77. Clough SJ, Bent AF. Floral dip: a simplified method for *Agrobacterium*-mediated transformation of *Arabidopsis thaliana*. Plant J. 1998;16:735-43.
78. Cui H, Ma H, Cui Y, Zhu X, Qin S, Li R. Cloning, identification and functional characterization of two cytochrome P450 carotenoids hydroxylases from the diatom *Phaeodactylum tricornutum*. J Biosci Bioeng. 2019;128:755-65.
79. Cui H, Ma H, Chen S, Yu J, Xu W, Zhu X, et al. Mitigating excessive ammonia nitrogen in chicken farm flushing wastewater by mixing strategy for nutrient removal and lipid accumulation in the green alga *Chlorella sorokiniana*. Bioresource Technol. 2020;303:122940.
80. Liu B, Sun Y, Xue J, Mao X, Jia X, Li R. Stearoyl-ACP$^{\Delta 9}$ desaturase 6 and 8 (GhA-SAD6 and GhD-SAD8) are responsible for biosynthesis of palmitoleic acid specifically in developing endosperm of upland cotton seeds. Front Plant Sci. 2019;10:703.
81. Bligh EG, Dyer WJ. A rapid method of total lipid extraction and purification. Can J Biochem Physiol. 1959;37:911-7.
82. Johansson MU, Zoete V, Michielin O, Guex N. Defining and searching for structural motifs using DeepView/Swiss-PdbViewer. BMC Bioinform. 2012;13:173.

Tables

Table 1 Primers used in experiment.

Primers	Sequence (5’-3’)
Homology cloning F1	GGTATTCAGCACATGNCYCAA
Homology cloning R1	TTGCCAAAGTGGTACACGSGCKC
Homology cloning F2	TGAGTTCCCTCACGGNGTGTYCC
Homology cloning R2	CCACCTCCACAAAGCCTNTGSGT
5’-RACE-R3	TGGTACACGGGCACCACT
5’-RACE-R4	CTCCACTGCCACCTCCACA
3’-RACE-F3	TGTTCCCGGACTTCAACAT
3’-RACE-F4	CATCCTCAGTGTTCTCAGT
ORF-F5	ATGGGTGTCGCAACGAATGCGA
ORF-R5	TCACTGGATCTCCAGCGGCTTGT
pYES2-F	GCATAACCACTTTAACTAATAC
pYES2-R	TCGGTTAGAGCGGATGTG
P1303-M13F	TGTAAAACGACGGCCAGT
P1303-M13R	CAGGAAACAGCTATGACC
NbActin-F	CAGTGGCCGTACAACAGGTA
NbActin-R	AACCGAAGAATTGCATGAGG
HaeDGAT2E-q-F6	GGGCRCCGTGGCGGTGATAG
HaeDGAT2E -q-R6	GCCTCGTTGCGGCTCGTCTT

Table 2 DGAT genes and GenBank accession numbers.

Gene name	Accession NO	Gene name	Accession NO
CzDGAT1A	QBG05553.1	CrDGAT1	XP_001692975.1
CzDGAT1B	QBG05554.1	CrDGAT2A	AGO32156.1
CzDGAT2A	QBG05555.1	CrDGAT2B	AGO32157.1
CzDGAT2B	QBG05556.1	CrDGAT2C	AGO32158.1
CzDGAT2C	QBG05557.1	CrDGAT2D	AGO32159.1
CzDGAT2D	QBG05558.1	CrDGAT2E	XP_001701667.1
CzDGAT2E	QBG05559.1	PtDGAT1	ADY76581.1
CzDGAT2F	QBG05560.1	PtDGAT2A	AFQ23659.1
CzDGAT2G	QBG05561.1	PtDGAT2B	AFM37314.1
CzDGAT2H	QBG05562.1	PtDGAT2C	AFQ23660.1
NoDGAT1A	ASL69957.1	PtDGAT2D	AFQ23661.1
NoDGAT1B	ASL69958.1	PtWSD	XP_002180007.1
NoDGAT2A	ATB53137.1	AtDGAT1	CAB45373.1
NoDGAT2B	ATB53138.1	AtDGAT2	NP_566952.1
NoDGAT2C	ATB53139.1	AtDGAT3	sp|Q9C5W0.2
NoDGAT2D	ATB53140.1	AtWSD	sp|Q93ZR6.1
NoDGAT2E	ATB53141.1	GmDGAT1A	BAE93460.1
NoDGAT2F	ATB53142.1	GmDGAT1B	NP_001237684.2
NoDGAT2G	ATB53143.1	GmDGAT1C	NP_001242457.1
NoDGAT2H	ATB53144.1	GmDGAT2D	K7K424.1
NoDGAT2I	ATB53145.1	GmDGAT3	XP_003542403.1
NoDGAT2J	ATB53146.1	GmWSD	XP_003552517.1
NoDGAT2K	ATB53136.1	UrDGAT2A	AAK84179.1
NoWSD	EWM29694.1	UrDGAT2B	AAK84180.1
Af293DGAT	EAL93134.1	AfDGAT	RMZ41827.1
TmDGAT	EEA25986.1	RmDGAT2B	CEG77579.1
MaDGAT	AQX34626.1		

Note: Cz (*Chromochloris zofingiensis*), Cr (*Chlamydomonas reinhardtii*), Pt (*Phaeodactylum tricornutum*), No (*Nannochloropsis oceanica*), At (*Arabidopsis thaliana*), Gm (*Glycine max*), Ur (*Umbelopsis ramanniana*), Af (*Aspergillus fumigatus Af293*), Tm (*Talaromyces marneffei ATCC*), Rm (*Rhizopus microsporus*), Ma (*Mortierella alpina*).

Figures

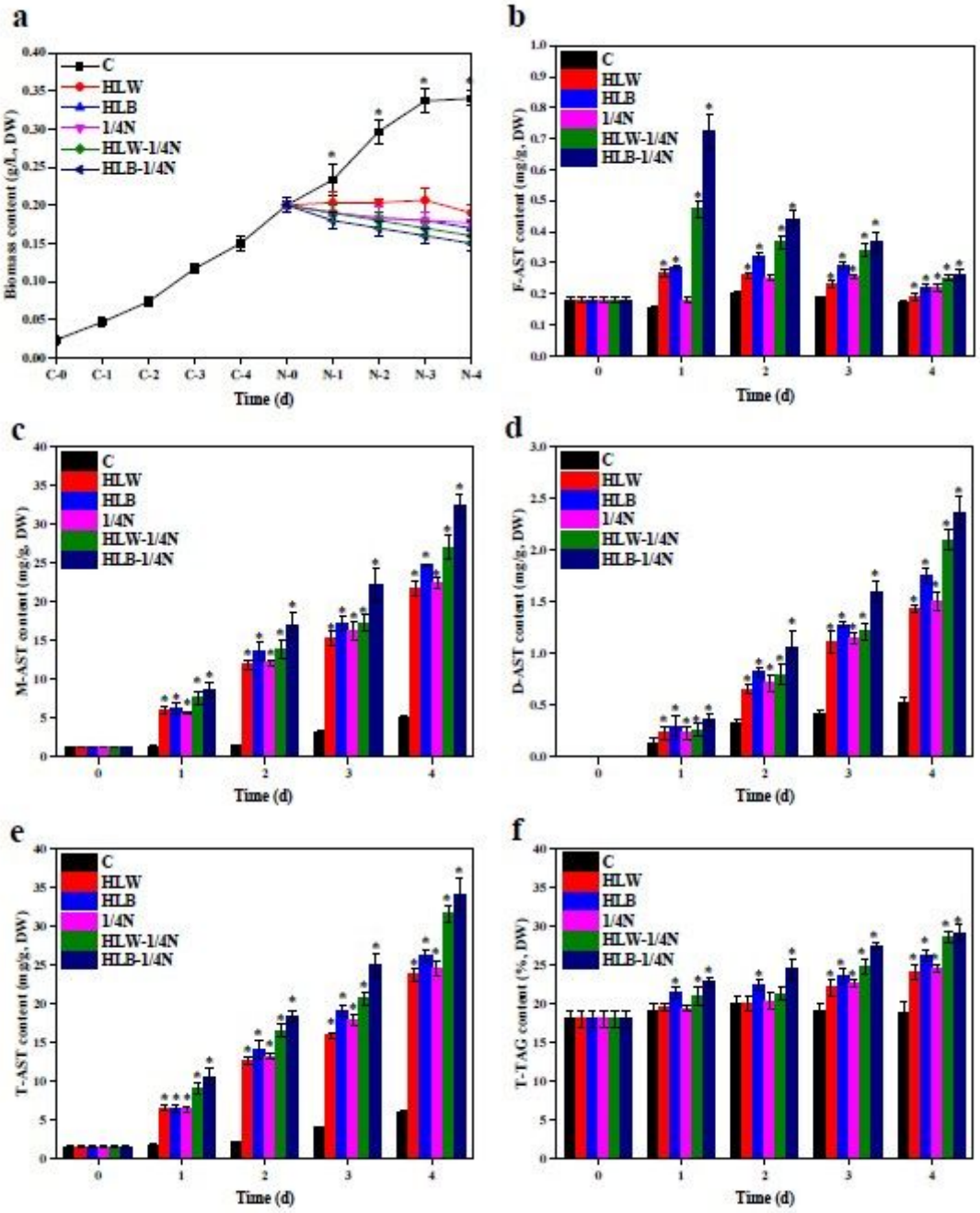

Figure 1

Growth, astaxanthin, and triacylglycerol profiles of Haematococcus lacustris under HLW, HLB, 1/4N, HLW-1/4N, and HLB-1/4N conditions after 1, 2, 3, and 4 day. (a) Time course of biomass content. (b) Free astaxanthin content. (c) Monoesterrified astaxanthin content. (d) Diesterrified astaxanthin content. (e) Total astaxanthin content. (f) Total triacylglycerol content.

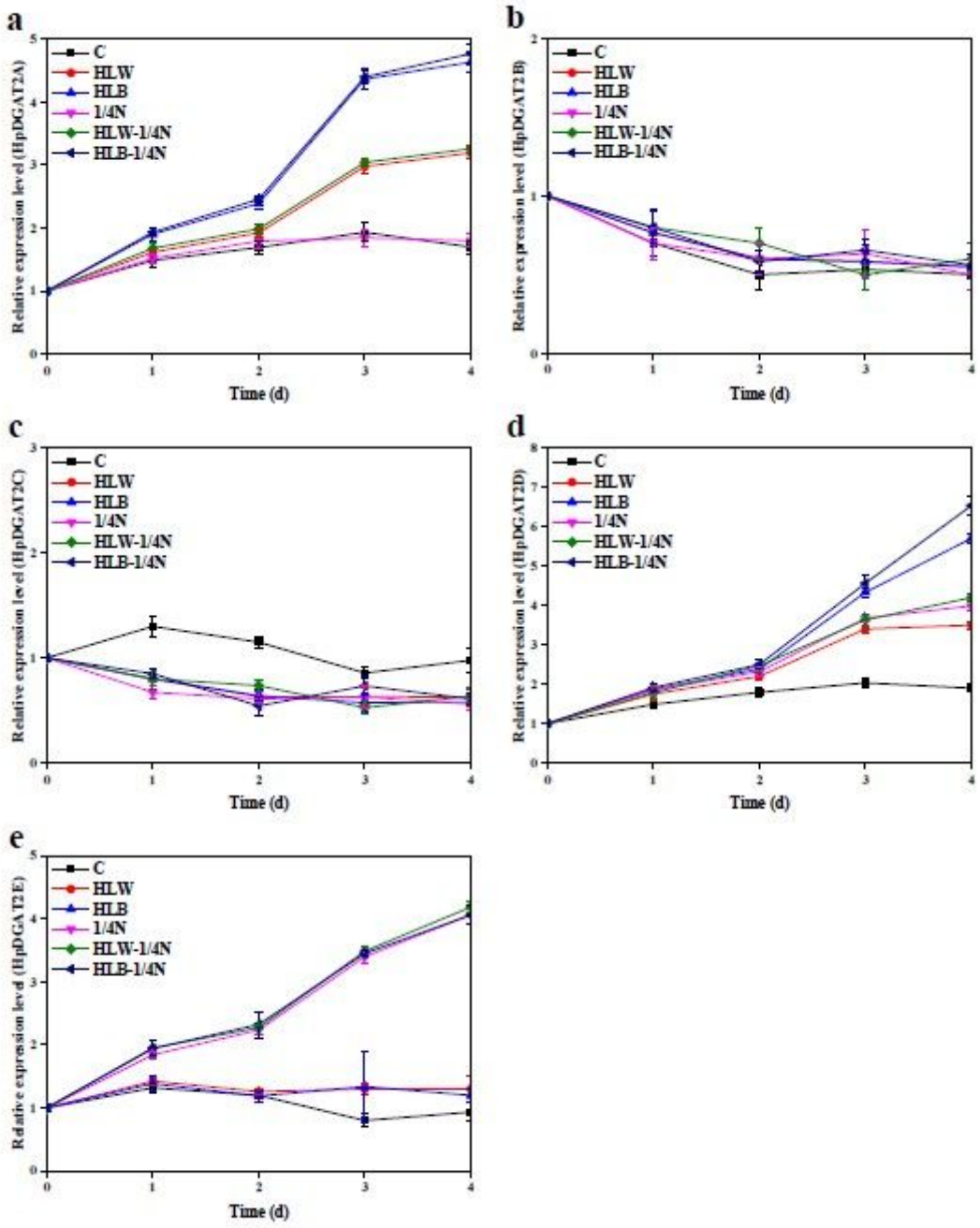

Figure 2

The transcriptional expression levels of HpDGAT2s in Haematococcus lacustris under HLW, HLB, 1/4N, HLW-1/4N, and HLB-1/4N conditions after 1, 2, 3, and 4 day. (a) HpDGAT2A. (b) HpDGAT2B. (c) HpDGAT2C. (d) HpDGAT2D. (e) HpDGAT2E. The gene expression levels were normalized to the endogenous ACTIN gene.

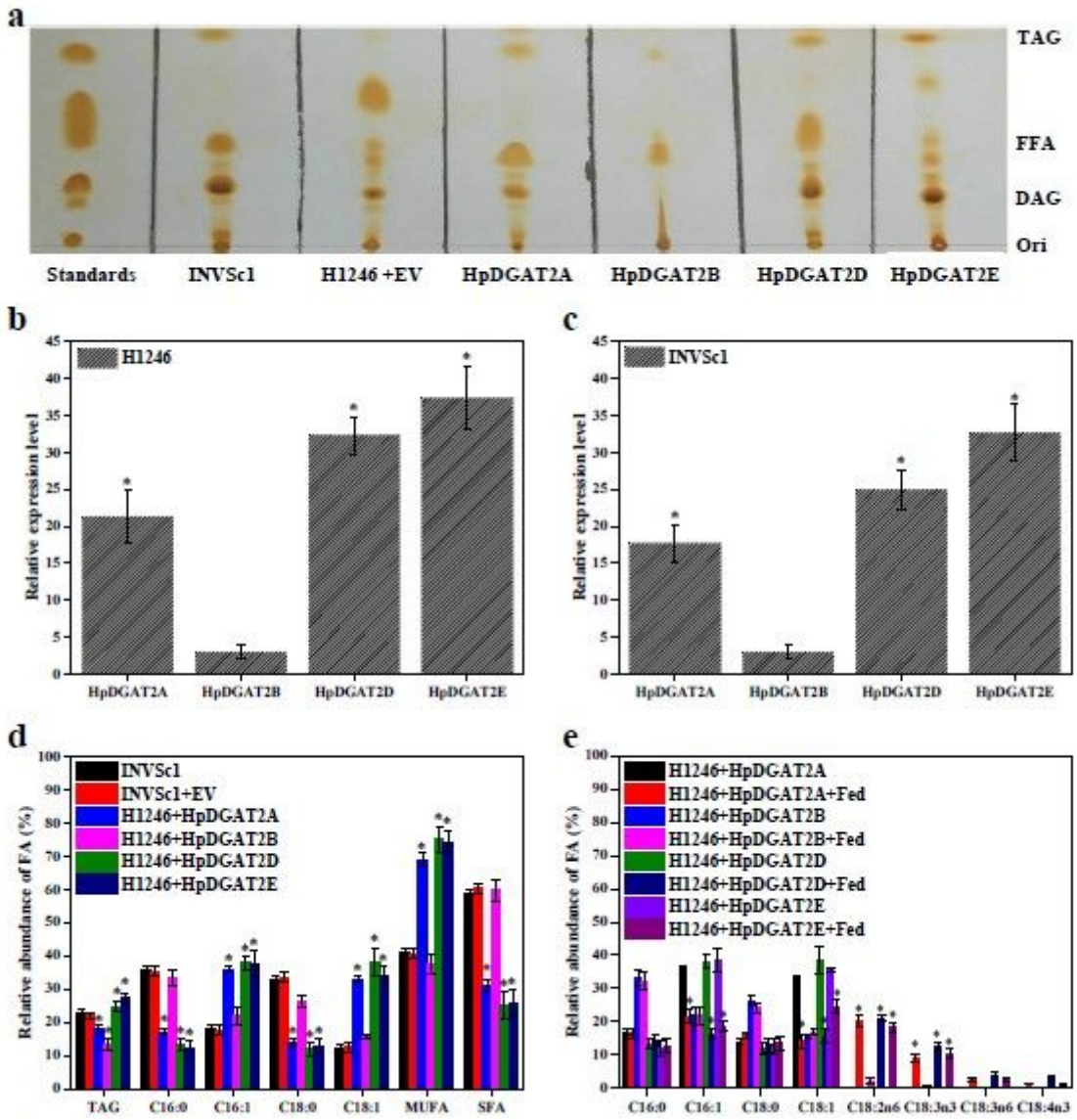

Figure 3

Functional characterization of HpDGAT2s in Saccharomyces cerevisiae cells. (a) TLC analysis of total lipids extracted from control S. cerevisiae (INVSc1), TAG-deficient S. cerevisiae (H1246), and H1246 cells transformed with HpDGAT2s and Empty vector (EV). (b) and (c) The transcriptional expression levels of HpDGAT2s in H1246 and INVSc1 cells transformed with HpDGAT2s. The gene expression levels were normalized to the endogenous ACT1 gene. (d) TAG contents and relative abundance of fatty acids in INVSc1 and H1246 cells transformed with HpDGAT2s. (e) Relative abundance of fatty acids in H1246 cells transformed with HpDGAT2s by the feeding of free fatty acids of C18:2n6, C18:3n3, C18:3n6, and C18:4n3 after a 24 h cultivation.

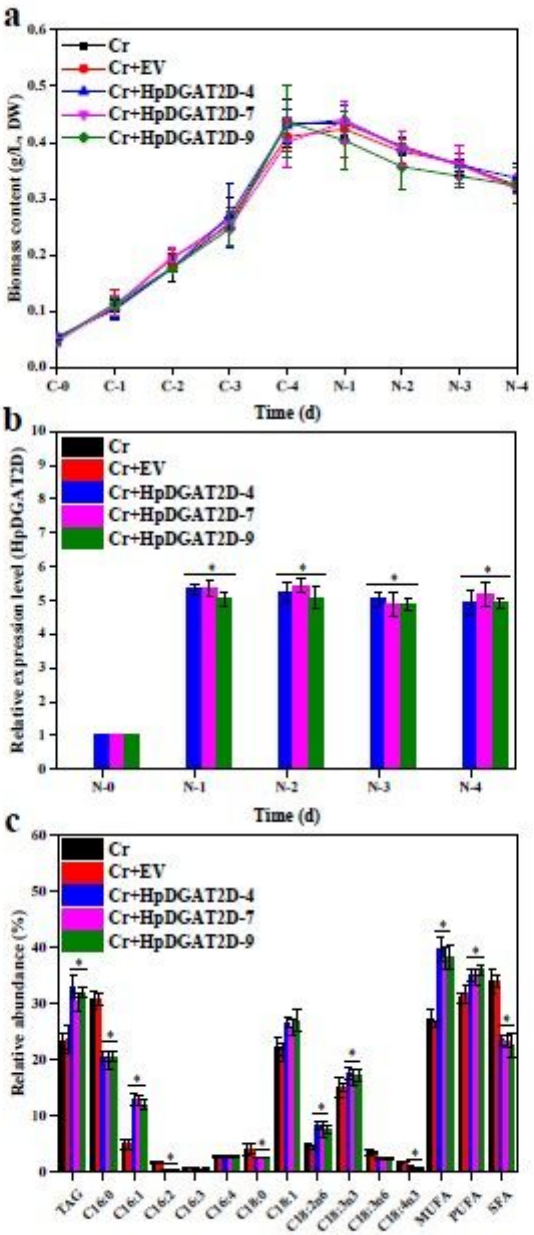

Figure 4

Overexpression of HpDGAT2Ds in Chlamydomonas reinhardtii cells. (a) Time course of biomass content under control and 1/4N conditions. (b) The transcriptional expression levels of HpDGAT2D in C. reinhardtii cells. The gene expression levels were normalized to the endogenous actin gene. (c) TAG contents and relative abundance of fatty acids in C. reinhardtii cells transformed with HpDGAT2D.

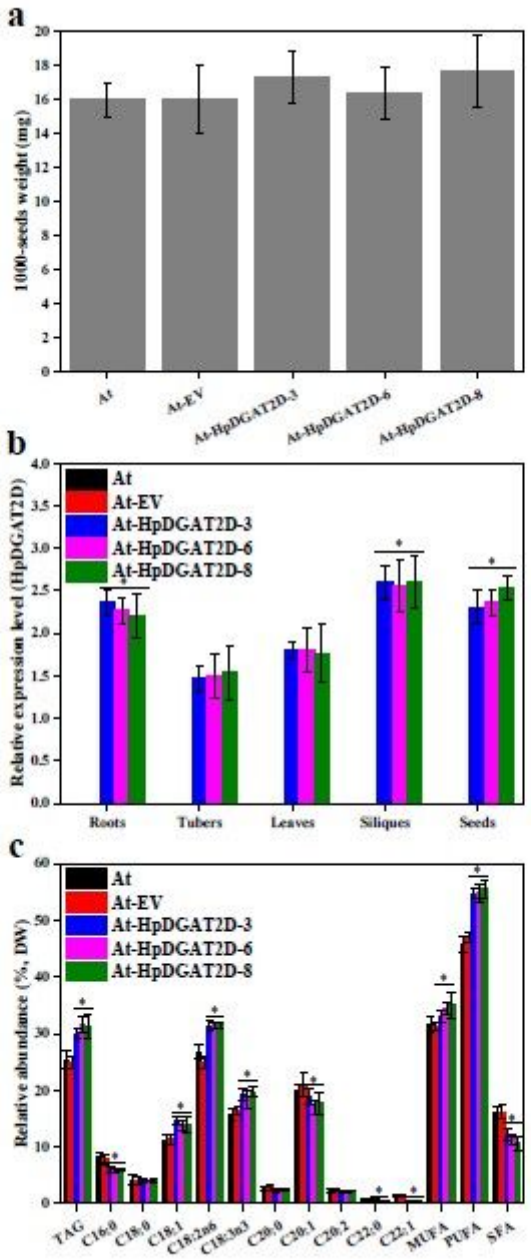

Figure 5

Overexpression of HpDGAT2Ds in Arabidopsis thaliana. (a) Average 1,000-seed weight (expressed as milligrams of weight/1,000 seeds) of transgenic Arabidopsis T4 seeds. (b) The transcriptional expression levels of HpDGAT2D in A. thaliana. The gene expression levels were normalized to the endogenous actin gene. (c) TAG contents and relative abundance of fatty acids in A. thaliana transformed with HpDGAT2D.

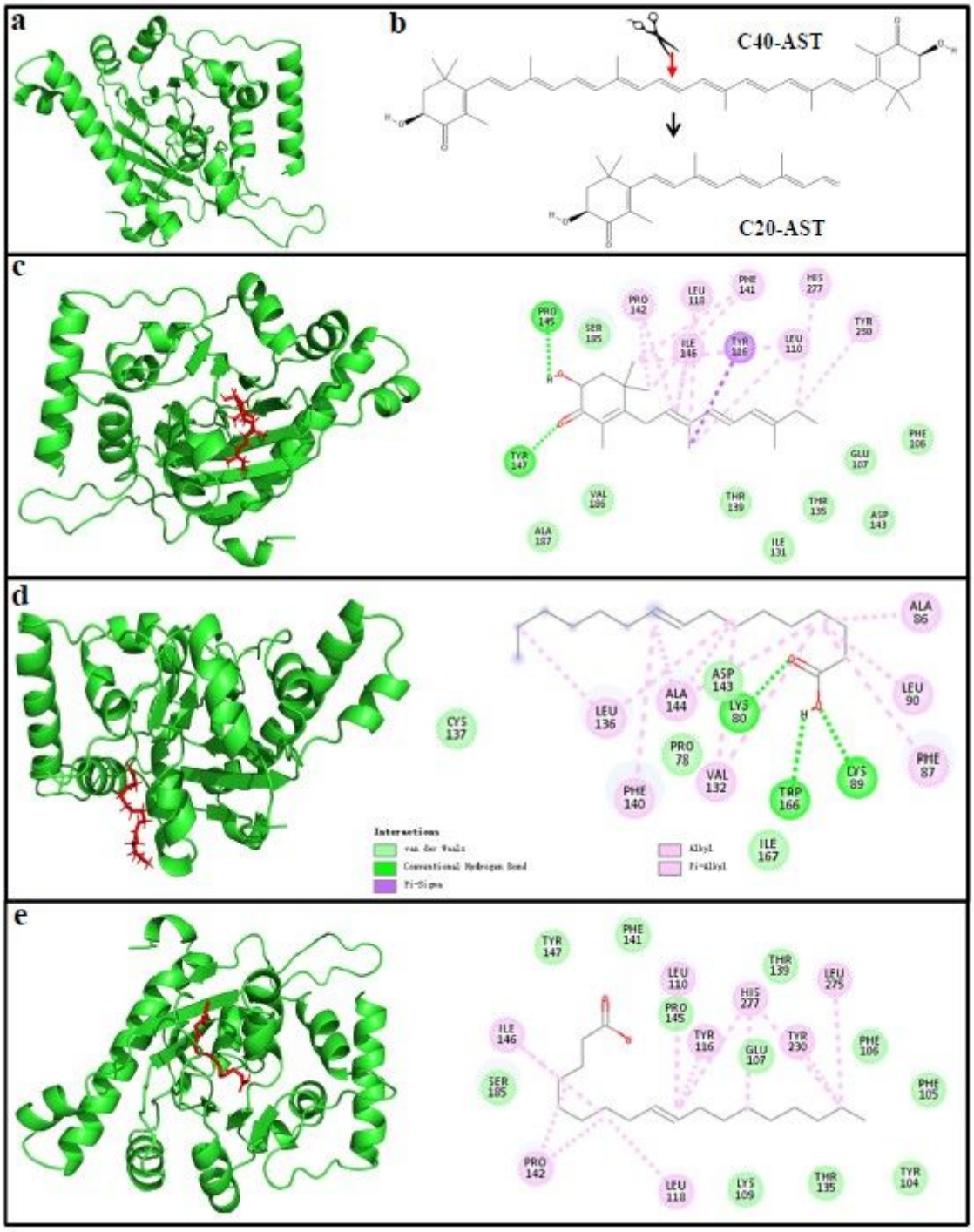

Figure 6

Docking of AST molecular and 3D model of HpDGAT2D using AutoDock software. (a) The 3D model of HpDGAT2D. (b) AST molecular. (c) Binding sites between AST and HpDGAT2D. (d) Binding sites between C16:1 and HpDGAT2D. (e) Binding sites between C18:1 and HpDGAT2D.

Supplementary Files

This is a list of supplementary files associated with this preprint. Click to download.

- Additionalfile112.pdf